

Unphysical poles and dispersion relations for Möbius domain-wall fermions in free field theory at finite L_s

Masaaki Tomii*

Physics Department, Columbia University, New York 10027, USA

(Received 14 July 2017; published 16 October 2017)

We find that the quark propagator constructed from the domain-wall fermion operator has $L_s - 1$ extra poles as well as the pole that realizes the physical quark in the continuum limit. We show the energy-momentum dispersion relation for the physical and unphysical poles of Möbius domain-wall fermions in free field theory at finite L_s . The dependence of extra pole energies on the Möbius parameter $b - c$ and on the domain-wall height M_5 is investigated. Our result suggests that small values of $b - c$ set a large lower bound on the unphysical pole masses and the contribution of these poles could be suppressed well by calculating with small $b - c$.

DOI: [10.1103/PhysRevD.96.074504](https://doi.org/10.1103/PhysRevD.96.074504)

I. INTRODUCTION

Introducing the charm quark into lattice simulation is desired to provide accurate Standard Model predictions for flavor physics, which enable us to probe for new physics beyond the Standard Model. Especially, the nonperturbative calculation of quantities associated with the Glashow-Iliopoulos-Maiani (GIM) mechanism [1] such as the $K_L - K_S$ mass difference (ΔM_K) essentially needs the charm quark to cancel the divergent contributions of up-quark loop diagrams. Because of the large charm-quark mass m_c compared to the typical scale of QCD, a lattice calculation including a charm quark encounters a scale problem. Namely, the lattice cutoff a^{-1} needs to be sufficiently larger than m_c to safely control the discretization error arising from am_c , while the box size L is usually required to obey $m_\pi L \gtrsim 4$, with the pion mass m_π , to avoid uncontrollable finite volume effects. Thus, lattice calculation at the physical pion and charm quark masses is a challenging task for the currently available computational resources.

This work is devoted to investigating properties of the discretization effects appearing in Möbius domain-wall fermions [2,3], an extension of Shamir domain-wall fermions [4,5], at heavy quark masses. Although the charm quark completely violates chiral symmetry due to its heavy mass, introducing the charm quark as a domain-wall fermion is still necessary to achieve an accurate GIM cancellation if the light quarks are implemented with a domain-wall fermion formulation, which appropriately preserves the chiral symmetry of the light quarks. There have been several works on D meson decay constants using domain-wall fermions [6,7] and overlap fermions for valence quarks and domain-wall fermions for sea quarks [8]. A lattice simulation including $2 + 1 + 1$ optimal domain-wall fermions [9] was implemented [10] and

was the first study with a dynamical domain-wall charm quark. In addition, the RBC and UKQCD collaborations are pursuing the calculation of the ΔM_K [11,12], ε_K [12,13], rare kaon decays $K \rightarrow \pi l^+ l^-$ [14,15], and $K \rightarrow \pi \nu \bar{\nu}$ [16,17], which are all associated with the GIM mechanism and quite sensitive to the discretization effects due to the charm-quark mass.

The charm quark treated in the domain-wall fermion formulation is supposed to have some special difficulties in addition to the naive $O(a^2 m_c^2)$ discretization errors and beyond. The seminal work on domain-wall fermions at large quark masses [18,19] investigated the Hermitian version of the domain-wall operator, the five-dimensional Dirac operator multiplied by the chirality operator γ_5 and the five-dimensional reflection operator. It found that the Hermitian operator contains unphysical modes of which the eigenvalues are largely independent of the input quark mass. This fact indicates that as the input quark mass approaches the cutoff the contribution of physical modes will be contaminated by unphysical modes.

This unphysical contribution may be related to the oscillatory behavior of domain-wall fermions [20], which is a particular issue of domain-wall fermions and is observed in correlation functions when a simulation is carried out at large domain-wall heights such as $M_5 \approx 1.7$. This unphysical oscillation was understood as the result of negative eigenvalues of the transfer matrix [21], which were shown to exist in the region of $M_5 > 1$ in the free field case.

Recently, another description of the origin of the unphysical oscillation was proposed [22,23]. The authors argued that the four-dimensional quark propagator constructed from the domain-wall fermion operator has an extra pole, the energy of which has a nonzero imaginary part $i\pi$ in lattice units for $M_5 > 1$ in free field theory, leading to an oscillatory behavior of the quark propagator. Their numerical result [23] indicates that the impact of the unphysical oscillation could be reduced by choosing M_5

*mt3164@columbia.edu

and the Möbius parameters b and c to satisfy $M_5(b-c) < 1$ and that the Borići domain-wall fermion [24] ($b = c$) is optimal to suppress the unphysical oscillation. Although this viewpoint of an unphysical pole is quite impressive and provides a clear interpretation of the unphysical effects of domain-wall fermions, we find that when examined in detail the authors' description [22,23] is not correct. Especially, we find there are $L_s - 1$ unphysical poles, while they found only one.

To motivate the presence of this collection of unphysical poles, it may be helpful to consider the case of overlap fermions, which has the same quark propagator as domain-wall fermions in the limit of infinite L_s up to a contact term and a normalization factor. The overlap Dirac operator is given by

$$D_{\text{ov}} = \frac{1}{2} + \frac{1}{2}\gamma_5 \frac{H}{\sqrt{H^2}}, \quad (1)$$

with a Hermitian kernel H . The corresponding propagator contains $\sqrt{H^2}$ and becomes ambiguous in the region where H^2 is not positive definite, resulting in the presence of an unphysical brunch cut for an imaginary value of Euclidean momentum variable p_4 . In this paper, we demonstrate the presence of $L_s - 1$ unphysical poles for finite L_s as the counterpart of this brunch cut.

We also examine the fundamental properties of the unphysical poles of domain-wall fermions by showing the dispersion relation for the physical and unphysical poles in free field theory at finite L_s . We find that the range of unphysical pole energies significantly depends on M_5 and $b - c$ as well as on the spatial momentum and that small values of $b - c$ set a large lower bound on the unphysical pole energies, possibly suppressing the contribution of the unphysical poles. Since this range of unphysical pole energies is found to be independent of the physical quark mass, numerical calculation with heavy quarks would be contaminated by unphysical poles as the physical quark mass approaches the lower bound of the unphysical pole region.

The paper is organized as follows. In Sec. II, we give definitions and some comments on the parameters of Möbius domain-wall fermions. In Sec. III, we give the five- and four-dimensional propagators of Möbius domain-wall fermions. In Sec. IV, we show the presence of unphysical poles of domain-wall fermions as well as the physical pole. In Sec. V, we show the dispersion relation for the physical and unphysical poles and discuss the dependence of unphysical pole energies on the parameters of Möbius domain-wall fermions. In Sec. VI, we conclude this paper and give some discussion. In Appendix A, we discuss a connection with overlap fermions and demonstrate that domain-wall fermions in the limit of infinite L_s and overlap fermions have an unphysical brunch cut instead of unphysical poles. In Appendix B, we give the five-

four-dimensional propagators in some special cases, in which the usual form of these propagators is irrelevant.

II. MÖBIUS DOMAIN-WALL FERMIONS

In this study, we work in the momentum space, where the lattice action of a Möbius domain-wall fermion is given by

$$S = \sum_{s,t=0}^{L_s-1} \sum_p \bar{\psi}_s(-p) (D_{\text{MDW}})_{s,t} \psi_t(p). \quad (2)$$

Here, $\bar{\psi}_s(-p)$ and $\psi_t(p)$ are the five-dimensional Möbius domain-wall fermion fields labeled by the four-dimensional momentum variables, $-p$ and p , and the indices for the fifth direction, $s, t = 0, 1, \dots, L_s - 1$. We employ the convention used by the RBC and UKQCD collaborations [25], in which the corresponding Dirac operator is defined by

$$D_{\text{MDW}} = \begin{pmatrix} \tilde{D} & -P_- & 0 & \dots & 0 & mP_+ \\ -P_+ & \tilde{D} & -P_- & \ddots & 0 & 0 \\ 0 & -P_+ & \tilde{D} & \ddots & \ddots & \vdots \\ \vdots & \ddots & \ddots & \ddots & -P_- & 0 \\ 0 & 0 & \ddots & -P_+ & \tilde{D} & -P_- \\ mP_- & 0 & \dots & 0 & -P_+ & \tilde{D} \end{pmatrix}. \quad (3)$$

Here, we define the chiral projection operators $P_{\pm} = \frac{1}{2}(1 \pm \gamma_5)$ and

$$\tilde{D} = D_-^{-1} D_+, \quad D_+ = 1 + bD_W, \quad D_- = 1 - cD_W, \quad (4)$$

with the Wilson Dirac operator D_W in the momentum space at a negative mass parameter $-M_5$,

$$D_W = i\tilde{\not{p}} + \sum_{\mu} (1 - \cos p_{\mu}) - M_5, \quad (5)$$

where $\tilde{\not{p}} = \sum_{\mu} \gamma_{\mu} \sin p_{\mu}$. For simplicity, we omit the lattice spacing a , and everything is expressed in lattice units throughout this paper.

We define the corresponding four-dimensional quark fields by

$$q = P_- \psi_0 + P_+ \psi_{L_s-1}, \quad \bar{q} = \bar{\psi}_0 P_+ + \bar{\psi}_{L_s-1} P_-. \quad (6)$$

As shown in Refs. [3,25], the four-dimensional quark propagator constructed from these fields $S_F^{4d}(p) = \langle q(-p) \bar{q}(p) \rangle$ in the limit $L_s \rightarrow \infty$ is the same as that in the corresponding overlap action up to a contact term and a normalization factor.

The action has five input parameters in total: the mass parameter m , the extent of the fifth dimension L_s , the domain-wall height M_5 , and the Möbius parameters b and c . Except for the mass parameter m , these are parameters of the regularization and do not affect any observables in the continuum limit. Therefore, we can tune them to minimize unwanted discretization effects. As is well known, the fifth-dimensional extent L_s determines the amount of violation of chiral symmetry on the lattice, which is usually quantified by the residual mass m_{res} and vanishes in the limit $L_s \rightarrow \infty$. The domain-wall height M_5 determines the scale for the exponential locality of the four-dimensional effective fermion field [26,27] and is also related to m_{res} [28]. The optimal choice of M_5 is 1 for the case of the free field, while that in the nonperturbative case has been studied by analyzing the spectral flow on some representative configurations to minimize m_{res} [28–31]. The obtained best choice was $M_5 = 1.7$ – 1.8 depending on the detail of the lattice setup. By applying link smearing, the residual mass may be better controlled, and the optimal choice of M_5 could be moved to 1 [32]. In addition, the M_5 dependence of the amount of discretization error for the heavy-heavy decay constant was investigated, resulting in a slightly smaller tuned value $M_5 = 1.6$ [33]. The Möbius scale $b + c$, which is proportional to the Möbius kernel, has also been tuned to minimize m_{res} , while the dependence on $b - c$ has not been studied a lot. In this work, we investigate how the significance of the unphysical modes depends on these parameters including $b - c$.

III. QUARK PROPAGATOR AT FINITE L_s

The five-dimensional Dirac operator D_{MDW} can be rewritten as

$$D_{\text{MDW}} = \frac{b+c}{D_-^\dagger D_-} i\tilde{p} + W^+ P_- + W^- P_+, \quad (7)$$

where

$$W_{s,t}^\pm = W\delta_{s,t} - \delta_{s\pm 1,t} + m\delta_{s/t,L_s-1}\delta_{t/s,0}, \quad (8)$$

$$W = \frac{-bc(\tilde{p}^2 + \mathcal{M}^2) + (b-c)\mathcal{M} + 1}{D_-^\dagger D_-}, \quad (9)$$

$$\mathcal{M} = \sum_\mu (1 - \cos p_\mu) - M_5, \quad (10)$$

$$D_-^\dagger D_- = c^2(\tilde{p}^2 + \mathcal{M}^2) - 2c\mathcal{M} + 1, \quad (11)$$

with $\tilde{p}^2 = \sum_\mu \sin^2 p_\mu$. Thus, we can calculate the five-dimensional propagator of Möbius domain-wall fermions in the same way [5] as for Shamir domain-wall fermions. We obtain

$$D_{\text{MDW}}^{-1} = \left[-\frac{b+c}{D_-^\dagger D_-} i\tilde{p} + W^- \right] G^- P_- + \left[-\frac{b+c}{D_-^\dagger D_-} i\tilde{p} + W^+ \right] G^+ P_+, \quad (12)$$

$$G^\pm = \left[\left(\frac{b+c}{D_-^\dagger D_-} \right)^2 \tilde{p}^2 + W^\mp W^\pm \right]^{-1} \equiv (Q^\pm)^{-1},$$

$$G_{s,t}^\pm = A_0 e^{-\alpha|s-t|} + A_\pm e^{\alpha(s+t-L_s+1)} + A_\mp e^{-\alpha(s+t-L_s+1)} + A_m \cosh[\alpha(s-t)], \quad (13)$$

$$\cosh \alpha = \frac{\left(\frac{b+c}{D_-^\dagger D_-} \right)^2 \tilde{p}^2 + W^2 + 1}{2W}, \quad (14)$$

$$A_0 = \frac{1}{2W \sinh \alpha}, \quad (15)$$

$$A_\pm = \frac{A_0}{F_{L_s}} (1 - m^2)(W - e^\mp \alpha), \quad (16)$$

$$A_m = \frac{A_0}{F_{L_s}} [4mW \sinh \alpha - 2(We^{-\alpha} - 1 + m^2(1 - We^\alpha))e^{-\alpha L_s}], \quad (17)$$

$$F_{L_s} = e^{\alpha L_s}(1 - We^\alpha + m^2(We^{-\alpha} - 1)) - 4mW \sinh \alpha + e^{-\alpha L_s}(We^{-\alpha} - 1 + m^2(1 - We^\alpha)). \quad (18)$$

Since the four-dimensional effective fields q and \bar{q} are given by (6), the four-dimensional quark propagator $S_F^{4d}(p) = \langle q(-p)\bar{q}(p) \rangle$ constructed from the Möbius domain-wall fermions is written as

$$S_F^{4d}(p) = P_- (D_{\text{MDW}}^{-1})_{0,0} P_+ + P_+ (D_{\text{MDW}}^{-1})_{L_s-1,L_s-1} P_- + P_- (D_{\text{MDW}}^{-1})_{0,L_s-1} P_- + P_+ (D_{\text{MDW}}^{-1})_{L_s-1,0} P_+ = \frac{2 \sinh(\alpha L_s)}{F_{L_s}} \frac{b+c}{D_-^\dagger D_-} i\tilde{p} + \frac{2}{F_{L_s}} \{ m[W \sinh(\alpha(L_s-1)) - \sinh(\alpha L_s)] - W \sinh \alpha \}. \quad (19)$$

In the limit of infinite L_s , this four-dimensional propagator becomes

$$S_F^{4d}(p) \xrightarrow{L_s \rightarrow \infty} \frac{\frac{b+c}{D_-^\dagger D_-} i\tilde{p} + m(We^{-\alpha} - 1)}{1 - We^\alpha + m^2(We^{-\alpha} - 1)}. \quad (20)$$

Since the Möbius scale $b + c$ is associated only with L_s dependence, the propagator in the limit of infinite L_s (20) must be independent of $b + c$, despite its apparent dependence on that combination. The $b + c$ -independent form is given in (A3).

The four-dimensional quark propagator (19) at finite L_s is quite different from that given in Ref. [23]. This may originate from the slight difference in F_{L_s} . Since the

coefficients (16) and (17) are determined through the boundary conditions (B5)–(B8) for the fifth direction, the validity of these coefficients and F_{L_s} given in this section can be checked by inserting $G_{s,t}^{\pm}$ into the boundary conditions.

IV. PHYSICAL AND UNPHYSICAL POLES AT FINITE L_s

It is well known that the quark propagator S_F^{4d} has a physical pole that reproduces an appropriate Dirac fermion in the continuum limit. This can be verified by expanding the denominator of the quark propagator with respect to the momentum variable. In the case of infinite L_s , the denominator of S_F^{4d} in (20) is expanded as

$$\begin{aligned} & 1 - We^\alpha + m^2(We^{-\alpha} - 1) \\ &= -\frac{(b+c)[M_5^2(2 - (b-c)M_5)^2 m^2 + p^2]}{M_5(2 - (b-c)M_5)(1 + cM_5)^2} \\ &+ O(p^4, m^2 p^2). \end{aligned} \quad (21)$$

Thus, the mass m_f^{pole} of the physical pole is approximated at $M_5(2 - (b-c)M_5)m$ for a light quark and is generally different from the input mass m even in the case of infinite L_s . In this work, we input m_f^{pole} and tune the parameter m to realize the pole mass m_f^{pole} .

Besides this physical pole, we find that F_{L_s} has other zero points, which could give an unphysical contribution to four-dimensional physics. Figure 1 shows $|F_{L_s} e^{-\alpha L_s}|^2$ calculated with Shamir domain-wall fermions at $L_s = 8$, $M_5 = 0.9$, $m_f^{\text{pole}} = 0.35$, $\vec{p} = 0$, and $\text{Re} p_4 = 0$. While the physical pole is seen at $\text{Im} p_4 = m_f^{\text{pole}} = 0.35$, there are nine other zero points of F_{L_s} . Two of them are trivially identified as the points satisfying $\cosh \alpha = 1$ or $\cosh \alpha = -1$, which correspond to $\text{Im} p_4 \approx 2.30$ and 0.74 in the plot, respectively. Between these two zero points, the seven other zero points are found. All of the zero points in this parameter choice are located on the imaginary axis of p_4 .

In Refs. [22,23], one of the trivial zero points satisfying $\cosh \alpha = 1$ was regarded as the unphysical pole of domain-wall fermions. However, the vanishing of F_{L_s} at $\cosh \alpha = \pm 1$ does not mean the presence of unphysical poles at these points because the numerator of the quark propagator (19) also vanishes at these points and one can verify the limit $\lim_{\alpha \rightarrow 0, i\pi} S_F^{4d}(p)$ is still finite. In fact, the original $L_s \times L_s$ matrix $Q^\pm = (G^\pm)^{-1}$ is still regular, $\det Q^\pm \neq 0$, even at these points. This confusion may originate from the fact that the functional form of the inverse matrix (13) is invalid for some special cases, $\cosh \alpha = \pm 1$ or $W = 0$, and the inverse matrix $G_{s,t}^{\pm}$ in these special cases has another functional form as given in Appendix B.

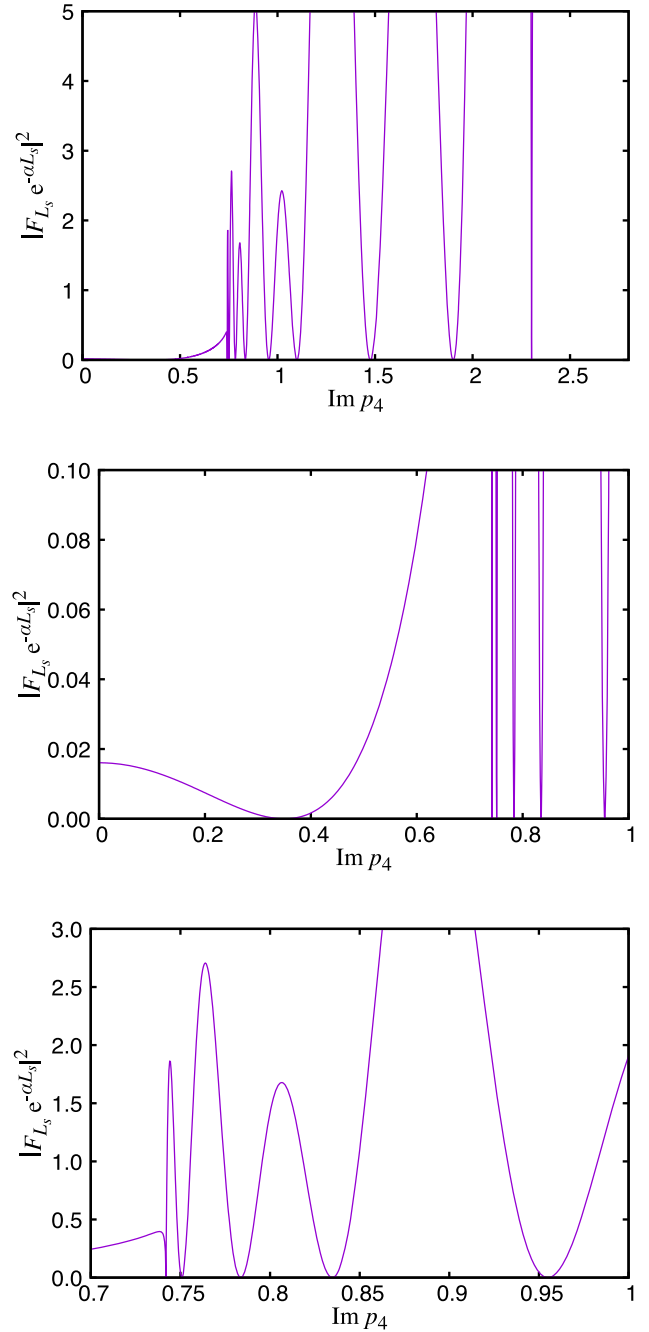


FIG. 1. $|F_{L_s} e^{-\alpha L_s}|^2$ calculated at $L_s = 8$, $M_5 = 0.9$, $m_f^{\text{pole}} = 0.35$, $b - c = 1$, $b + c = 1$, $\vec{p} = 0$, and $\text{Re} p_4 = 0$ plotted as a function of $\text{Im} p_4$. The lower two panels are magnifications of complicated parts in the top panel, which accommodates all the zero points of F_{L_s} .

The quark propagator at each of the remaining seven zero points between these special zero points has a real singularity. These zero points may give a significant lattice artifact when the calculation is done at a large value of m_f^{pole} . We regard these zero points as the unphysical poles. Note that these unphysical poles are located in the region $-1 < \cosh \alpha < 1$, in which α is pure imaginary and any

terms in (18) are not suppressed at large L_s , showing some oscillatory behavior with varying $\text{Im} p_4$. As the extent of the fifth direction L_s increases, the number of these oscillations also increases, leading to the presence of more unphysical poles. In our analysis, there are always $L_s - 1$ unphysical poles. In the limit of infinite L_s , an unphysical branch cut appears instead of a series of unphysical poles as shown in Appendix A.

In the following section, we discuss the fundamental properties of these unphysical poles by showing the energy-momentum dispersion relation at various input parameters.

V. DISPERSION RELATIONS

As mentioned in the previous section, the quark propagator (19) at finite L_s has $L_s - 1$ unphysical poles as well as the physical pole. In this section, we discuss the properties of the unphysical poles and the best choice of the Möbius parameters to suppress them by analyzing the dispersion relation for these poles in free field theory. While it is likely familiar to the reader, for completeness, we point out that, although lattice calculations are performed in Euclidean space with $\vec{p}^2 = \sum_\mu \sin^2 p_\mu > 0$, it is the location of poles at negative values of p_4^2 that determines the physical energies $E(\vec{p}) = \text{Im} p_4(\vec{p})$ of the quark states in free field theory. These poles and corresponding energies determine the exponential falloff of the quark propagators at large Euclidean time separations. The dispersion relation for fermions on the lattice deviate from those for continuum fermions with $O(a^2)$ error. While dispersion relations for improved overlap fermions using the Brillouin kernel were investigated [32,34], we concentrate on the dispersion relations for unimproved Möbius domain-wall fermions to investigate another source of cutoff effects due to unphysical poles.

Figure 2 shows the dispersion relation for the domain-wall fermion at $M_5 = 0.9$, $L_s = 8$, $m_f^{\text{pole}} = 0$, $b = 1$, and $c = 0$. The spatial momentum is chosen in the diagonal direction, $\vec{p} = (\frac{|\vec{p}|}{\sqrt{3}}, \frac{|\vec{p}|}{\sqrt{3}}, \frac{|\vec{p}|}{\sqrt{3}})$. In the figure, one physical (solid curve) and seven unphysical poles (dashed curves) are seen on the imaginary axis of p_4 at any spatial momentum.

As discussed in the previous section, these unphysical poles are confined to the region between two curves, $\cosh \alpha = 1$ (dashed-dotted curve) and $\cosh \alpha = -1$ (dotted curve). The boundaries $\cosh \alpha = \pm 1$ are analytically given by

$$\cos p_4|_{\cosh \alpha = 1} = \frac{\sum_{i=1}^3 \sin^2 p_i + B^2 + 1}{2B}, \quad (22)$$

$$\begin{aligned} \cos p_4|_{\cosh \alpha = -1} &= \frac{4 + 4(b-c)B + (b-c)^2(\sum_{i=1}^3 \sin^2 p_i + B^2 + 1)}{4(b-c) + 2(b-c)^2 B}, \end{aligned} \quad (23)$$

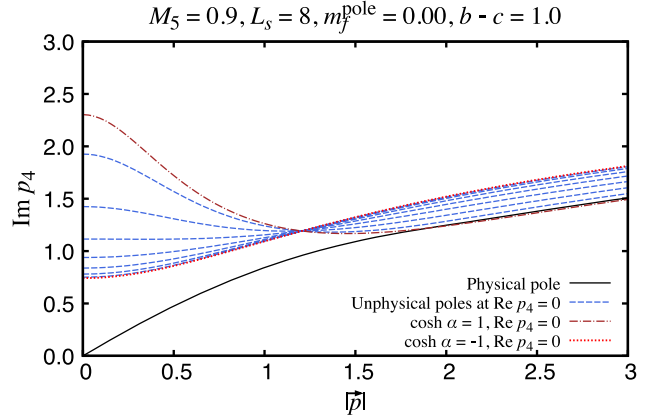


FIG. 2. Dispersion relation for the domain-wall fermion at $M_5 = 0.9$, $L_s = 8$, $m_f^{\text{pole}} = 0$, $b + c = 1$, $b - c = 1$, and spatial momentum $\vec{p} = (\frac{|\vec{p}|}{\sqrt{3}}, \frac{|\vec{p}|}{\sqrt{3}}, \frac{|\vec{p}|}{\sqrt{3}})$.

$$B = 4 - M_5 - \sum_{i=1}^3 \cos p_i. \quad (24)$$

The solution of $\cosh \alpha = 1$ depends only on M_5 and p_i , implying that either of the corresponding lower or upper bounds on the unphysical pole locations depends only on M_5 . On the other hand, the solution of $\cosh \alpha = -1$ depends also on $b - c$, and therefore the other bound on the unphysical pole masses could be controlled by varying $b - c$. Since $b + c$ is not related to the region of unphysical pole energies and is usually tuned to minimize the residual mass, we fix $b + c = 1$ and do not vary it in this work.

Before varying M_5 and $b - c$, which play a key role to change the region of unphysical pole energies, we briefly present the results of varying the other parameters m_f^{pole} and L_s . In Fig. 3, we show the dispersion relation in a massive case at $m_f^{\text{pole}} = 0.35$. While the physical pole mass has certainly moved to 0.35, the unphysical poles remain at close to their earlier locations when $m_f^{\text{pole}} = 0$. In fact, the

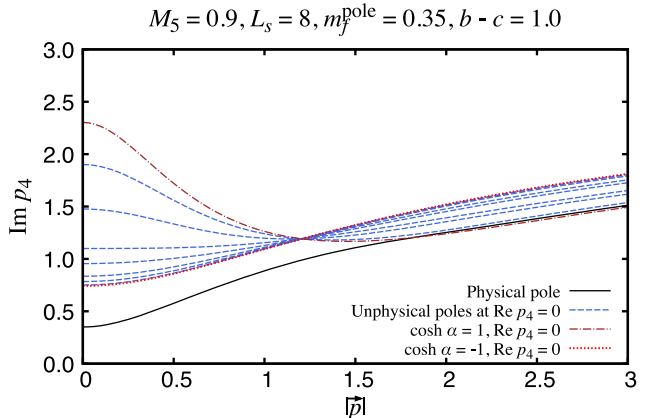


FIG. 3. Same as Fig. 2 but at $m_f^{\text{pole}} = 0.35$.

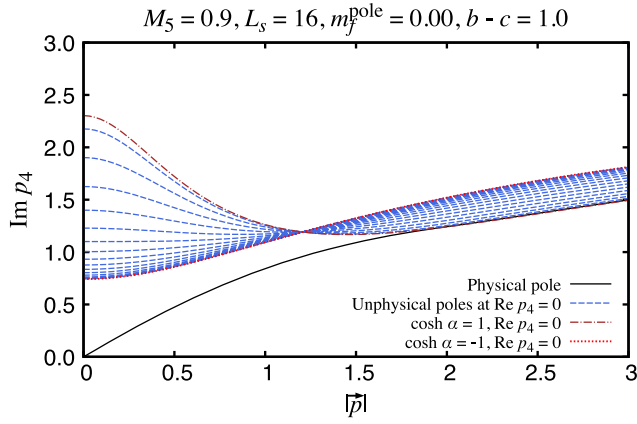


FIG. 4. Same as Fig. 2 but at $L_s = 16$.

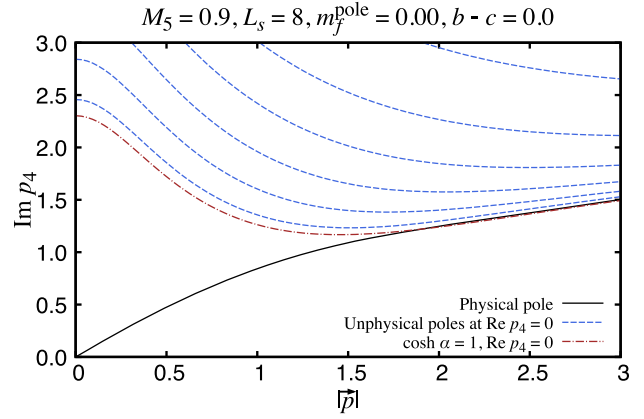


FIG. 6. Same as Fig. 2 but at $b - c = 0$.

boundaries (22), (23) of the unphysical poles are independent of m_f^{pole} . Therefore, as the physical pole mass m_f^{pole} increases and approaches the unphysical pole masses, the dominance of the physical pole would be lost. A similar observation was shown in Refs. [18,19], which investigated the physical and unphysical modes of the Hermitian version of the five-dimensional operator, the Dirac operator multiplied by γ_5 , and the reflection operator.

Figure 4 shows the dispersion relation at $L_s = 16$ and with the same values of the other parameters as those in Fig. 2. As described in the previous section, F_{L_s} oscillates in the region $-1 < \cosh \alpha < 1$ with varying the momentum variable, and its frequency is proportional to L_s . Thus, the number of unphysical poles has been increased to 15.

Now, we show the results at smaller values of $b - c$. Figure 5 shows the result at $b - c = 0.5$. The values of $\text{Im} p_4$ on the curve $\cosh \alpha = -1$ are larger than those for the Shamir type $b - c = 1$, and the lower bound on the unphysical pole masses has been increased to ~ 1.41 . This fact implies that the contribution of unphysical poles at long distances would be suppressed more rapidly. Figure 6 shows the result at $b - c = 0$, where $\text{Im} p_4$ with

$\cosh \alpha = -1$ is infinitely large as (23) indicates. Thus, small values of $b - c$ make the unphysical modes heavy and realize a small coupling between unphysical poles and the four-dimensional physics.

So far, we have discussed in the case of $M_5 = 0.9 < 1$, which has the most simple structure of unphysical poles. The case $M_5 = 1$ gives a similar dispersion relation with a slight modification that $\text{Im} p_4$ with $\cosh \alpha = 1$ diverges at $\vec{p} = 0$ as described by (22).

In the case of $M_5 > 1$, α could be pure imaginary at $\text{Re} p_4 = \pi$ as well as at $\text{Re} p_4 = 0$, and therefore some of the unphysical poles are located at $\text{Re} p_4 = \pi$. Figure 7 shows the result at $M_5 = 1.4$. The curve of $\cosh \alpha = 1$ (dashed-dotted curve) on the imaginary axis blows up at $|\vec{p}| \approx 0.90$, below which the solution of $\cosh \alpha = 1$ (dashed double-dotted curve) is located at $\text{Re} p_4 = \pi$. Thus, there are some unphysical poles at $\text{Re} p_4 = \pi$ (coarse-dashed curves) at small spatial momenta. As suggested in Refs. [22,23], this kind of unphysical pole may cause unphysical oscillation because the contribution of an unphysical pole at $p_4 = p_4^{\text{pole}}$ to the quark propagator for the time direction has a term $\sim e^{i p_4^{\text{pole}} x_4}$, which is oscillatory unless $\text{Re} p_4^{\text{pole}} = 0$.

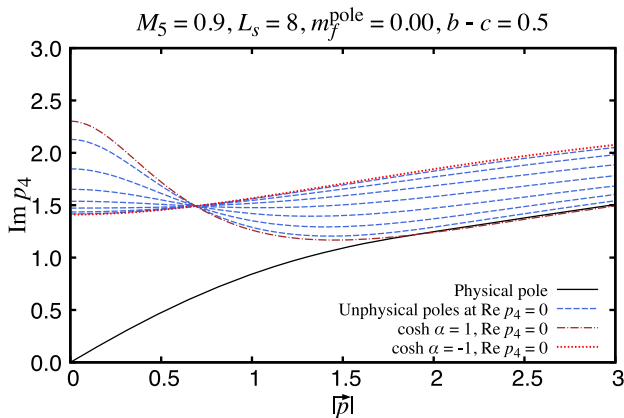


FIG. 5. Same as Fig. 2 but at $b - c = 0.5$.

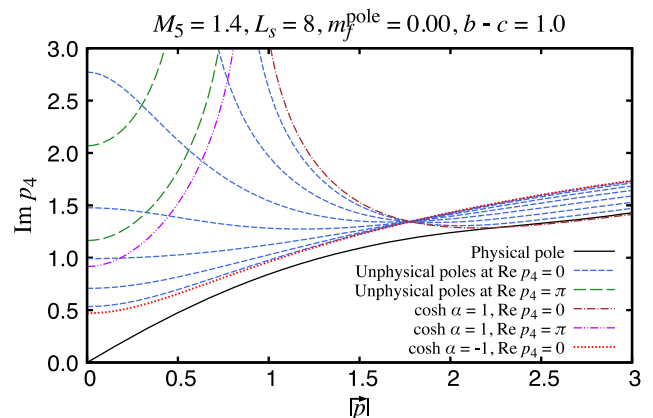
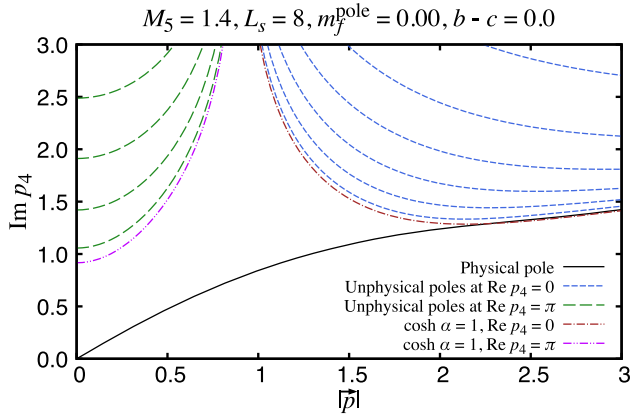


FIG. 7. Same as Fig. 2 but at $M_5 = 1.4$.

FIG. 8. Same as Fig. 7 but at $b - c = 0$.

In Fig. 7, the lower bound on the unphysical pole masses at $\text{Re} p_4 = 0$ is smaller than that at $\text{Re} p_4 = \pi$, implying that the unphysical contributions from the former poles are more significant than those from the latter poles. Figure 8 shows the result at $b - c = 0$. Although the unphysical poles on the imaginary axis of p_4 at small spatial momenta have certainly disappeared by taking $b - c = 0$, all unphysical poles have entered the region of $\text{Re} p_4 = \pi$, the lower limit (22) of which can be increased only by changing M_5 .

We close this section with some comments on the choice of domain-wall parameters. As we have seen, taking small $b - c$ plays a crucial role in reducing the contribution of unphysical poles by increasing the lower bound on their masses. In fact, the oscillatory behavior of domain-wall fermions [20], which is supposed to be due to the unphysical poles, has never been observed in the case of $b - c = 0$, while that for $b - c = 1$ is quite visible at large values of M_5 .

The lower bound on the unphysical pole masses is determined by the solution of $\cosh \alpha = -1$ (23) if $b - c$ satisfies

$$b - c > \frac{2(1 - M_5)}{1 - (1 - M_5)^2} \quad \text{for } M_5 < 1,$$

$$b - c > \frac{2(M_5 - 1)}{1 + (M_5 - 1)^2} \quad \text{for } M_5 > 1. \quad (25)$$

At small values of $b - c$ that do not satisfy the inequality (25), the lower bound is determined by the solution of $\cosh \alpha = 1$ (22), which is independent of $b - c$ and depends only on M_5 . This fact provides two prospects. One is that taking extremely small $b - c$ compared to the threshold in (25) may not have a strong advantage. The other is that M_5 may also need to be chosen appropriately to suppress the unphysical contribution. Obviously, the choice $M_5 = 1$ is optimal in free field theory. In the mean field approximation [22,35], the optimal choice is

modified to $M_5 = 4 - 3u_0$ with u_0 being the averaged link variable.

It is also important to take into account the violation of chiral symmetry of the light quarks due to finite L_s . The parameters $b + c$ and M_5 are usually tuned to minimize the residual mass, while the dependence on $b - c$ has not been investigated a lot. Note that small values of $b - c$, which are desired to reduce the contribution of the unphysical poles, set a large upper limit on the eigenvalues of the Möbius kernel, potentially resulting in an inappropriate approximation to the sign function. Thus, the parameters b , c , and M_5 need to be carefully tuned in nonperturbative studies so that both the residual mass and the contribution of unphysical poles are safely small.

VI. CONCLUSION

This study is dedicated to the exploration of a new way to precisely calculate heavy-quark physics using Möbius domain-wall fermions. Our strategy is to treat the charm quark with the same regularization as the lighter quarks without applying any effective theory or changing any discretization parameters to achieve an appropriate GIM cancellation. We have concentrated on a serious discretization error for heavy quarks that originates from the unphysical poles of domain-wall fermions by analyzing the energy-momentum dispersion relation.

As we have shown, the quark propagator constructed from domain-wall fermions has $L_s - 1$ unphysical poles, and their energies are strongly dependent on the difference of the Möbius parameters $b - c$ as well as on the domain-wall height M_5 . The lower bound on the unphysical pole masses in the case of $b - c = 1$ is usually smaller than the lattice cutoff and quite comparable to the charm-quark mass on lattices at currently available lattice spacings. We demonstrated that this lower bound can be increased by taking $b - c$ smaller.

One concern is that small $b - c$ could increase the residual mass because the upper limit on the eigenvalues of the Möbius kernel increases as $b - c$ decreases, potentially spoiling the accuracy of the approximated sign function. We therefore need to tune the parameters, taking account of the residual breaking of chiral symmetry as well as of the impact of unphysical poles. A nonperturbative study to explore the best choice of these parameters is ongoing.

ACKNOWLEDGMENTS

I thank the members of the RBC and UKQCD collaborations and Katsumasa Nakayama for useful discussions and comments. I also express my gratitude to Norman Christ and Raza Sufian for careful reading of the manuscript. This work is supported in part by U.S. DOE Grant No. DE-SC0011941.

APPENDIX A: UNPHYSICAL BRANCH CUT IN INFINITE L_s

In this Appendix, we demonstrate what happens in the limit of infinite L_s . First of all, it is important to note that the four-dimensional quark propagator for infinite L_s is supposed to be independent of $b + c$ because $b + c$ is associated only with L_s dependence, while (20) does apparently contain $b + c$. We can show (20) is independent of $b + c$ as follows. Since the limit (20) is valid only if $\text{Re}\alpha > 0$ on the real axis of p_4 , we can identify

$$\sinh \alpha = \frac{(b+c)\sqrt{FG}}{WD_-^\dagger D_-}, \quad (\text{A1})$$

where we define

$$F = \frac{\tilde{p}^2 + \mathcal{M}^2}{2}, \quad G = \frac{(b-c)^2 \tilde{p}^2 + (2 + (b-c)\mathcal{M})^2}{2}. \quad (\text{A2})$$

In the case of $W < 0$, $\sinh \alpha$ is negative for $\text{Re}\alpha > 0$ because $\cosh \alpha$ is also negative and α has an imaginary part $i\pi$. Inserting $e^{\pm\alpha} = \cosh \alpha \pm \sinh \alpha$ into (20), we obtain

$$\lim_{L_s \rightarrow \infty} S_F^{4d} = - \frac{i\tilde{p} + m(\mathcal{M} + (b-c)F - \sqrt{FG})}{(1-m^2)(\mathcal{M} + (b-c)F) + (1+m^2)\sqrt{FG}}. \quad (\text{A3})$$

Thus, the four-dimensional quark propagator in the limit of infinite L_s is independent of $b + c$.

Since there are square roots of FG in (A3), some ambiguity could occur in the region where FG is not positive definite. This ambiguity could be interpreted as the presence of an unphysical branch cut. In fact, F and G vanish at p_4 , satisfying $\cosh \alpha = 1$ (22) and $\cosh \alpha = -1$ (23), respectively, and the product FG is negative between these two points. Thus, a series of unphysical poles at finite L_s becomes an unphysical branch cut in the limit of infinite L_s . The quark propagator at finite L_s does not contain such a branch cut because the insertion of $e^{\pm\alpha} = \cosh \alpha \pm \sinh \alpha$ to (19) cancels the square roots.

The propagator (A3) can be derived also from the Dirac operator of overlap fermions, which is defined by

$$D_{\text{ov}} = \frac{1+m}{2} + \frac{1-m}{2} \gamma_5 \frac{H_M}{\sqrt{H_M^2}}. \quad (\text{A4})$$

Here, we use the Möbius kernel

$$H_M = \gamma_5 \frac{(b+c)D_W}{2 + (b-c)D_W}. \quad (\text{A5})$$

The inverse matrix of D_{ov} is found to be

$$D_{\text{ov}}^{-1} = \frac{(1-m)(-i\tilde{p} + \mathcal{M} + (b-c)F) + (1+m)\sqrt{FG}}{(1-m^2)(\mathcal{M} + (b-c)F) + (1+m^2)\sqrt{FG}} \quad (\text{A6})$$

and obeys

$$\lim_{L_s \rightarrow \infty} S_F^{4d} = \frac{D_{\text{ov}}^{-1} - 1}{1-m}. \quad (\text{A7})$$

Therefore, overlap fermions have the same unphysical effects as domain-wall fermions.

APPENDIX B: PROPAGATOR IN SOME SPECIAL CASES

In this paper, we wrote the explicit form of G^\pm , the inverse of the matrix

$$Q^\pm = \left(\frac{b+c}{D_-^\dagger D_-} \right)^2 \tilde{p}^2 + W^\mp W^\pm. \quad (\text{B1})$$

The components of Q^\pm are given by

$$\begin{aligned} Q_{s,t}^\pm &= \left[\left(\frac{b+c}{D_-^\dagger D_-} \right)^2 \tilde{p}^2 + W^2 + 1 \right] \delta_{s,t} - W(\delta_{s+1,t} + \delta_{s-1,t}) \\ &\quad + mW(\delta_{s,L_s-1} \delta_{t,0} + \delta_{s,0} \delta_{t,L_s-1}) - (1-m^2) \\ &\quad \times \begin{cases} \delta_{s,0} \delta_{t,0} (+) \\ \delta_{s,L_s-1} \delta_{t,L_s-1} (-) \end{cases}. \end{aligned} \quad (\text{B2})$$

The inverse matrix $G^\pm = (Q^\pm)^{-1}$ satisfies the recurrence relations

$$\left[\left(\frac{b+c}{D_-^\dagger D_-} \right)^2 \tilde{p}^2 + W^2 + 1 \right] G_{s,t}^\pm - W(G_{s+1,t}^\pm + G_{s-1,t}^\pm) = \delta_{s,t}, \quad (\text{B3})$$

$$\left[\left(\frac{b+c}{D_-^\dagger D_-} \right)^2 \tilde{p}^2 + W^2 + 1 \right] G_{s,t}^\pm - W(G_{s,t+1}^\pm + G_{s,t-1}^\pm) = \delta_{s,t}, \quad (\text{B4})$$

and the boundary conditions

$$WG_{-1,t}^+ - (1-m^2)G_{0,t}^+ + mWG_{L_s-1,t}^+ = 0, \quad (\text{B5})$$

$$G_{L_s,t}^+ + mG_{0,t}^+ = 0, \quad (\text{B6})$$

$$mG_{L_s-1,t}^- + G_{-1,t}^- = 0, \quad (\text{B7})$$

$$WG_{L_s,t}^- - (1-m^2)G_{L_s-1,t}^- + mWG_{0,t}^- = 0. \quad (\text{B8})$$

The solution for the usual case is already given in (13). In the following, we give $G_{s,t}^\pm$ and the corresponding

four-dimensional quark propagator S_F^{4d} in the special cases, $W = 0$, $\cosh \alpha = 1$, and $\cosh \alpha = -1$.

1. $W = 0$

In this case, the matrices Q^\pm are given by

$$Q_{s,t}^+ = \left[\left(\frac{b+c}{D_-^\dagger D_-} \right)^2 \tilde{p}^2 + 1 \right] \delta_{s,t} - (1-m^2) \delta_{s,0} \delta_{t,0}, \quad (\text{B9})$$

$$Q_{s,t}^- = \left[\left(\frac{b+c}{D_-^\dagger D_-} \right)^2 \tilde{p}^2 + 1 \right] \delta_{s,t} - (1-m^2) \delta_{s,L_s-1} \delta_{t,L_s-1}. \quad (\text{B10})$$

The corresponding inverse matrices are

$$G_{s,t}^+ = \left[\left(\frac{b+c}{D_-^\dagger D_-} \right)^2 \tilde{p}^2 + 1 \right]^{-1} \delta_{s,t} (1 - \delta_{s,0}) + \left[\left(\frac{b+c}{D_-^\dagger D_-} \right)^2 \tilde{p}^2 + m^2 \right]^{-1} \delta_{s,0} \delta_{t,0}, \quad (\text{B11})$$

$$G_{s,t}^- = \left[\left(\frac{b+c}{D_-^\dagger D_-} \right)^2 \tilde{p}^2 + 1 \right]^{-1} \delta_{s,t} (1 - \delta_{s,L_s-1}) + \left[\left(\frac{b+c}{D_-^\dagger D_-} \right)^2 \tilde{p}^2 + m^2 \right]^{-1} \delta_{s,L_s-1} \delta_{t,L_s-1}, \quad (\text{B12})$$

which correspond to the four-dimensional quark propagator

$$S_F^{4d} = \frac{-\frac{b+c}{D_-^\dagger D_-} \mathbf{i}\tilde{\mathcal{P}} + m}{\left(\frac{b+c}{D_-^\dagger D_-} \right)^2 \tilde{p}^2 + m^2}. \quad (\text{B13})$$

2. $\cosh \alpha = 1$

In this case, the recurrence relations (B3) and (B4) are

$$\begin{aligned} 2WG_{s,t}^\pm - W(G_{s+1,t}^\pm + G_{s-1,t}^\pm) &= \delta_{s,t}, \\ 2WG_{s,t}^\pm - W(G_{s,t+1}^\pm + G_{s,t-1}^\pm) &= \delta_{s,t}, \end{aligned} \quad (\text{B14})$$

the solution of which is formally given by

$$G_{s,t}^\pm = -\frac{|s-t|}{2W} + C_{2,\pm}^{(1)} st + C_{s,\pm}^{(1)} s + C_{t,\pm}^{(1)} t + C_{0,\pm}^{(1)}. \quad (\text{B15})$$

The boundary conditions (B5)–(B8) determine the coefficients,

$$C_{2,+}^{(1)} = C_{2,-}^{(1)} = -\frac{1}{WF_{L_s}^{(1)}} (1-m^2)(1-W), \quad (\text{B16})$$

$$C_{s,+}^{(1)} = C_{t,+}^{(1)} = \frac{1}{2WF_{L_s}^{(1)}} (1-m^2)((1-W)L_s + W), \quad (\text{B17})$$

$$C_{s,-}^{(1)} = C_{t,-}^{(1)} = \frac{1}{2WF_{L_s}^{(1)}} (1-m^2)((1-W)L_s + W - 2), \quad (\text{B18})$$

$$C_{0,+}^{(1)} = -\frac{L_s}{F_{L_s}^{(1)}}, \quad (\text{B19})$$

$$C_{0,-}^{(1)} = -\frac{1}{WF_{L_s}^{(1)}} (WL_s - (1-m^2)(L_s - 1)), \quad (\text{B20})$$

$$F_{L_s}^{(1)} = (1-m^2)(1-W)L_s - W(1+m)^2. \quad (\text{B21})$$

The corresponding four-dimensional propagator is given by

$$\begin{aligned} S_F^{4d} &= \frac{b+c}{D_-^\dagger D_-} \frac{L_s}{F_{L_s}^{(1)}} \mathbf{i}\tilde{\mathcal{P}} - \frac{L_s m(1-W) + (1+m)W}{F_{L_s}^{(1)}} \\ &\xrightarrow{L_s \rightarrow \infty} \frac{\frac{b+c}{D_-^\dagger D_-} \mathbf{i}\tilde{\mathcal{P}} - m(1-W)}{(1-m^2)(1-W)} = -\frac{\mathbf{i}\tilde{\mathcal{P}} - m\mathcal{M}}{(1-m^2)\mathcal{M}}. \end{aligned} \quad (\text{B22})$$

The inverse matrix $G_{s,t}^\pm$ and the four-dimensional quark propagator S_F^{4d} derived in this subsection can be reproduced also from the limit $\alpha \rightarrow 0$ of $G_{s,t}^\pm$ and S_F^{4d} in the standard case (13), (19), (20).

3. $\cosh \alpha = -1$

The recurrence relations (B3) and (B4) in this case are

$$\begin{aligned} -2WG_{s,t}^\pm - W(G_{s+1,t}^\pm + G_{s-1,t}^\pm) &= \delta_{s,t}, \\ -2WG_{s,t}^\pm - W(G_{s,t+1}^\pm + G_{s,t-1}^\pm) &= \delta_{s,t}, \end{aligned} \quad (\text{B23})$$

the solution of which is formally given by

$$G_{s,t}^\pm = \left(\frac{|s-t|}{2W} + C_{2,\pm}^{(-1)} st + C_{s,\pm}^{(-1)} s + C_{t,\pm}^{(-1)} t + C_{0,\pm}^{(-1)} \right) (-1)^{s-t}. \quad (\text{B24})$$

In the case of even L_s , the coefficients are

$$C_{2,+}^{(-1)} = C_{2,-}^{(-1)} = \frac{1}{WF_{L_s}^{(-1)}} (1-m^2)(1+W), \quad (\text{B25})$$

$$C_{s,+}^{(-1)} = C_{t,+}^{(-1)} = -\frac{1}{2WF_{L_s}^{(-1)}} (1-m^2)((1+W)L_s - W), \quad (\text{B26})$$

$$C_{s,-}^{(-1)} = C_{t,-}^{(-1)} = -\frac{1}{2WF_{L_s}^{(-1)}} (1-m^2)((1+W)L_s - W - 2), \quad (\text{B27})$$

$$C_{0,+}^{(-1)} = -\frac{L_s}{F_{L_s}^{(-1)}}, \quad (\text{B28})$$

$$C_{0,-}^{(-1)} = -\frac{1}{WF_{L_s}^{(-1)}}(WL_s + (1 - m^2)(L_s - 1)), \quad (\text{B29})$$

$$F_{L_s}^{(-1)} = (1 - m^2)(1 + W)L_s + W(1 + m)^2. \quad (\text{B30})$$

The corresponding four-dimensional propagator is given by

$$\begin{aligned} S_F^{4d} &= \frac{b+c}{D_-^\dagger D_-} \frac{L_s}{F_{L_s}^{(-1)}} i\tilde{p} - \frac{L_s m(1+W) - (1+m)W}{F_{L_s}^{(-1)}} \\ &\xrightarrow{L_s \rightarrow \infty} \frac{\frac{b+c}{D_-^\dagger D_-} i\tilde{p} - m(1+W)}{(1-m^2)(1+W)} \\ &= -\frac{2i\tilde{p} + m(2\mathcal{M} + (b-c)(\tilde{p}^2 + \mathcal{M}^2))}{(1-m^2)(2\mathcal{M} + (b-c)(\tilde{p}^2 + \mathcal{M}^2))}. \end{aligned} \quad (\text{B31})$$

$G_{s,t}^\pm$ and S_F^{4d} derived in this subsection can be reproduced also from the limit $\alpha \rightarrow i\pi$ of $G_{s,t}^\pm$ and S_F^{4d} in the standard case (13), (19), (20).

-
- [1] S. L. Glashow, J. Iliopoulos, and L. Maiani, Weak interactions with lepton-hadron symmetry, *Phys. Rev. D* **2**, 1285 (1970).
- [2] R. C. Brower, H. Neff, and K. Orginos, Möbius fermions: Improved domain wall chiral fermions, *Nucl. Phys. B, Proc. Suppl.* **140**, 686 (2005).
- [3] R. C. Brower, H. Neff, and K. Orginos, The Möbius domain wall fermion algorithm, *Comput. Phys. Commun.* **220**, 1 (2017).
- [4] D. B. Kaplan, A method for simulating chiral fermions on the lattice, *Phys. Lett. B* **288**, 342 (1992).
- [5] Y. Shamir, Chiral fermions from lattice boundaries, *Nucl. Phys.* **B406**, 90 (1993).
- [6] W.-P. Chen, Y.-C. Chen, T.-W. Chiu, H.-Y. Chou, T.-S. Guu, and T.-H. Hsieh (TWQCD Collaboration), Decay constants of pseudoscalar D -mesons in lattice QCD with domain-wall fermion, *Phys. Lett. B* **736**, 231 (2014).
- [7] P. A. Boyle, L. Del Debbio, A. Juttner, A. Khamseh, F. Sanfilippo, and J. T. Tsang, The decay constants f_D and f_{D_s} in the continuum limit of $N_f = 2 + 1$ domain wall lattice QCD, [arXiv:1701.02644](https://arxiv.org/abs/1701.02644).
- [8] Y.-B. Yang *et al.*, Charm and strange quark masses and f_{D_s} from overlap fermions, *Phys. Rev. D* **92**, 034517 (2015).
- [9] T.-W. Chiu, Optimal Domain Wall Fermions, *Phys. Rev. Lett.* **90**, 071601 (2003).
- [10] Y.-C. Chen and T.-W. Chiu (TWQCD Collaboration), Lattice QCD with $N_f = 2 + 1 + 1$ domain-wall quarks, *Phys. Lett. B* **767**, 193 (2017).
- [11] Z. Bai, N. H. Christ, T. Izubuchi, C. T. Sachrajda, A. Soni, and J. Yu, $K_L - K_S$ Mass Difference from Lattice QCD, *Phys. Rev. Lett.* **113**, 112003 (2014).
- [12] N. Christ, T. Izubuchi, C. T. Sachrajda, A. Soni, and J. Yu (RBC and UKQCD Collaborations), Calculating the $K_L - K_S$ mass difference and ϵ_K to sub-percent accuracy, *Proc. Sci.*, LATTICE2013 (2014) 397.
- [13] Z. Bai, Long distance part of ϵ_K from lattice QCD, *Proc. Sci.*, LATTICE2016 (2017) 309.
- [14] N. H. Christ, X. Feng, A. Portelli, and C. T. Sachrajda (RBC and UKQCD Collaborations), Prospects for a lattice computation of rare kaon decay amplitudes: $K \rightarrow \pi \ell^+ \ell^-$ decays, *Phys. Rev. D* **92**, 094512 (2015).
- [15] N. H. Christ, X. Feng, A. Juttner, A. Lawson, A. Portelli, and C. T. Sachrajda, First exploratory calculation of the long-distance contributions to the rare kaon decays $K \rightarrow \pi \ell^+ \ell^-$, *Phys. Rev. D* **94**, 114516 (2016).
- [16] N. H. Christ, X. Feng, A. Portelli, and C. T. Sachrajda (RBC and UKQCD Collaborations), Prospects for a lattice computation of rare kaon decay amplitudes II $K \rightarrow \pi \nu \bar{\nu}$ decays, *Phys. Rev. D* **93**, 114517 (2016).
- [17] Z. Bai, N. H. Christ, X. Feng, A. Lawson, A. Portelli, and C. T. Sachrajda, Exploratory Lattice QCD Study of the Rare Kaon Decay $K^+ \rightarrow \pi^+ \nu \bar{\nu}$, *Phys. Rev. Lett.* **118**, 252001 (2017).
- [18] G.-f. Liu, Ph.D. thesis, Columbia University, New York, 2003.
- [19] N. H. Christ and G. Liu, Massive domain wall fermions, *Nucl. Phys. B, Proc. Suppl.* **129**, 272 (2004).
- [20] J. J. Dudek, R. G. Edwards, and D. G. Richards, Radiative transitions in charmonium from lattice QCD, *Phys. Rev. D* **73**, 074507 (2006).
- [21] S. Syritsyn and J. W. Negele, Oscillatory terms in the domain wall transfer matrix, *Proc. Sci.*, LAT2007 (2007) 078.
- [22] J. Liang, Y. Chen, M. Gong, L.-C. Gui, K.-F. Liu, Z. Liu, and Y.-B. Yang, Oscillatory behavior of the domain wall fermions revisited, *Phys. Rev. D* **89**, 094507 (2014).
- [23] R. S. Sufian, M. J. Glatzmaier, and Y.-B. Yang, Unphysical Poles of Domain Wall Fermions at finite L_s , [arXiv:1603.01591](https://arxiv.org/abs/1603.01591).
- [24] A. Borici, Truncated overlap fermions, *Nucl. Phys. B, Proc. Suppl.* **83**, 771 (2000).
- [25] T. Blum *et al.* (RBC and UKQCD Collaborations), Domain wall QCD with physical quark masses, *Phys. Rev. D* **93**, 074505 (2016).
- [26] P. Hernandez, K. Jansen, and M. Luscher, Locality properties of Neuberger's lattice Dirac operator, *Nucl. Phys.* **B552**, 363 (1999).
- [27] Y. Kikukawa and Y. Nakayama, Gauge anomaly cancellations in $SU(2)_L U(1)_Y$ electroweak theory on the lattice, *Nucl. Phys.* **B597**, 519 (2001).

- [28] Y. Aoki *et al.*, Domain wall fermions with improved gauge actions, *Phys. Rev. D* **69**, 074504 (2004).
- [29] D. J. Antonio *et al.* (RBC and UKQCD Collaborations), Localization and chiral symmetry in three flavor domain wall QCD, *Phys. Rev. D* **77**, 014509 (2008).
- [30] P. Hagler *et al.* (LHPC Collaboration), Nucleon generalized parton distributions from full lattice QCD, *Phys. Rev. D* **77**, 094502 (2008).
- [31] A. Walker-Loud *et al.*, Light hadron spectroscopy using domain wall valence quarks on an Asqtad sea, *Phys. Rev. D* **79**, 054502 (2009).
- [32] Y.-G. Cho, S. Hashimoto, A. Jüttner, T. Kaneko, M. Marinkovic, J.-I. Noaki, and J. T. Tsang, Improved lattice fermion action for heavy quarks, *J. High Energy Phys.* **05** (2015) 072.
- [33] P. Boyle, A. Jüttner, M. K. Marinkovic, F. Sanfilippo, M. Spraggs, and J. T. Tsang, An exploratory study of heavy domain wall fermions on the lattice, *J. High Energy Phys.* **04** (2016) 037.
- [34] S. Durr and G. Koutsou, On the suitability of the Brillouin action as a kernel to the overlap procedure, [arXiv:1701.00726](https://arxiv.org/abs/1701.00726).
- [35] S. Aoki and Y. Taniguchi, One loop calculation in lattice QCD with domain wall quarks, *Phys. Rev. D* **59**, 054510 (1999).